Journal of Catalysis **205,** 339–345 (2002)
doi:10.1006/jcat.2001.3461, available online at http://www.idealibrary.com on IDEAL®

Temperature-Programmed Reaction Spectroscopy of Ceria- and Cu/Ceria-Supported Oxide Catalyst

P. Zimmer,[1] A. Tschöpe, and R. Birringer

Universität des Saarlandes, FR 7.3 Technische Physik, 66123 Saarbrücken, Germany

Received July 9, 2001; revised October 26, 2001; accepted November 2, 2001; published online January 3, 2002

The surface reduction and oxidation of nanocrystalline CeO_2 and CuO/CeO_2 was investigated by temperature-programmed reduction (TPR) and isothermal/temperature-programmed oxidation (TPO) measurements. Samples with Cu concentrations in the range of 5–20% were prepared by homogeneous precipitation and characterized with regard to their composition, structure, and specific surface area. The quantitative analysis of H_2 TPR measurements of the mixed oxides indicated that (i) the majority of the copper component was completely reduced at temperatures below 473 K and (ii) chemisorption of hydrogen occurred at $T = 375$ K, catalyzed by the copper oxide. The reoxidation of the samples with N_2O could also be separated into two partial reactions: (i) a reaction of N_2O with adsorbed hydrogen at room temperature and (ii) the oxidation of the reduced copper component between 343 and 573 K. Annealing of $Cu_{0.08}Ce_{0.92}O_{2-x}$ at temperatures above 1073 K resulted in the precipitation of a copper oxide phase, as was evident from X-ray diffraction (XRD). Changes in the morphology of the copper component, induced by high-temperature annealing, had a significant effect on the N_2O TPO profile even after annealing at temperatures below 1073 K, where XRD was not sensitive.

Key Words: **temperature-programmed reduction (TPR); temperature-programmed oxidation (TPO); ceria; copper oxide; morphology.**

1. INTRODUCTION

Cerium oxide is known as an active catalyst for oxidation reactions (1, 2). The activity for oxidation of carbon monoxide can be significantly increased by doping with transition metals. It has been reported that among various dopants, the system CuO/CeO_2 exhibited the highest activity for CO oxidation (3), even comparable with the activity of commercial precious metal catalysts (4). Investigations into the activity of copper oxide supported on CeO_2 and γ-Al_2O_3 catalysts for NO conversion showed an enhanced activity of CuO/CeO_2 compared to CuO/γ-Al_2O_3 (5). Another important reaction in which CuO/CeO_2 exhibits high catalytic activity is the total oxidation of methane (3, 6). This particular reaction has recently attracted new attention since the mixture CuO/CeO_2 is apparently well suited for use as electrodes in solid oxide fuel cells involving the direct conversion of hydrocarbons (7). The high activity of CuO/CeO_2 raises questions with regard to the atomic, chemical, and electronic structure of this material. X-ray diffraction (XRD) (8) and scanning transmission electron microscopy (9) revealed that the copper component in $Cu_{0.15}Ce_{0.85}O_{2-x}$ prepared using magnetron sputtering (10) was highly dispersed on the surface of CeO_2 nanocrystals. Thermal stability of the dispersion was only limited by sintering of the ceria support, indicating a rather strong chemical interaction between the support and the copper component. This chemical affinity was also verified by electrochemical measurements (11). The copper chemical potential was reduced as compared to the known copper oxide phases, indicating a solid solution. Taking into account the low solubility of copper in the cerium oxide bulk phase, the experimentally observed apparent solubility of 15 at% was associated with a surface layer of copper–cerium mixed oxide (11). Further studies by X-ray photoelectron spectroscopy showed that the copper component in the intimate mixture with cerium oxide could be readily reduced and oxidized at temperatures as low as 473 K (12). The copper valencies were found to be Cu^0, Cu^{1+}, and Cu^{2+}, depending on the reduction and oxidation conditions. The major objective of the present study was to investigate how the distinct oxidation and reduction properties of both copper and cerium oxide combine in the surface layer of nanostructured CuO/CeO_2 catalysts. As an experimental approach, samples of various copper concentration or different specific surface area were analyzed using quantitative H_2 temperature-programmed reduction (TPR) and isothermal or temperature-programmed oxidation (TPO) with N_2O. Nitrous oxide has often been used to measure specifically the copper surface area by selective chemisorption, thus allowing quantification of copper dispersion in supported catalyst (13, 15). However, earlier pulsed oxidation measurements of CuO/CeO_2 materials aiming at a characterization of the copper dispersion in the supported metal catalyst failed in so far as unphysical dispersions of more than 100% were obtained for the copper component.

[1] To whom correspondence should be addressed. Fax: +49 (0)681/302-5222. E-mail: P.Zimmer@nano.uni-saarland.de.

0021-9517/02 $35.00

It was a second objective of the present study to identify the origin of this failure and to find out whether a modified experimental procedure would provide the desired information on the morphology of the copper component.

2. EXPERIMENTAL

2.1. Sample Preparation

CeO_2 and CuO/CeO_2 were prepared by a homogeneous precipitation method using hexamethylenetetramine (HMT) (16). Two aqueous solutions of 0.0375 M cerium (III)nitrate and 0.5 M HMT were mixed and stirred at room temperature for 24 h. The precipitate was centrifuged, washed twice with 2-propanole, and dried at 343 K. A further heat treatment in air at 623 K for at least 30 min was performed in order to completely oxidize the precipitate and to remove organic residues. The mixed CuO/CeO_2 oxides were prepared by adding a defined amount of copper (II) nitrate to the cerium nitrate solution. By varying the copper nitrate concentration in the precursor solution, it was possible to prepare mixed oxide samples with Cu concentrations in the range of 5–20 mol%.

The preparation of samples with different surface area was realized by annealing in 8% O_2/Ar for 2 h. In the case of CuO/CeO_2, the samples were taken from the same batch of mixed oxide powder so that the compositions of the specimens were identical whereas the specific surface areas after annealing at 873, 973, 1073, and 1173 K were different.

2.2. Characterization

Surface area and structure. The specific area of the samples were obtained from nitrogen adsorption isothermes at $T = 77$ K using a Micromeritics ASAP 2010. The analysis of the isotherms was performed using the supported DFT-plus software (17, 18). The advantage of this analysis as compared to the BET method is that condensation in micropores, which are present in the nanocrystalline cerium oxide samples, are explicity taken into account. Assuming a pore-size distribution function $f(H)$ the adsorption isotherm is described as a superposition $Q(p) = \sum dH q(p, H) f(H)$ of model isotherms $q(p, H)$, which were obtained from density functional theory (DFT). The unknown pore-size distribution function $f(H)$ is received by a least-squares fit of experimental isotherms. With an asumption for the pore geometry, the total surface area of the samples can be determined.

X-ray diffraction measurements were performed in order to identify the crystalline phases of the oxide samples. A Siemens D-500 diffractometer with Cu $K\alpha$ radiation and a primary LiF-monochromator was employed.

Chemical composition. The chemical compositions of the CuO/CeO_2 samples were measured using the energy-dispersive X-ray analysis of a JEOL JXA 840 A scanning electron microscope. The chemical analysis was calibrated by measuring a series of standard samples of known composition.

Surface reduction and oxidation. The reduction and oxidation measurements were performed using a vertical fixed-bed reactor in a tube furnace. Samples of 0.2 g of pure cerium oxide or 0.15 g of CuO/CeO_2 were placed between two layers of quartz granules inside a quartz tube. A reaction gas flow of 50 sccm downward from the reactor was stabilized by mass flow controllers. The TPR and TPO measurements were performed at a heating rate of 10 K min^{-1}. The reactive gas compositions were 5% H_2/Ar for TPR and 5% N_2O/Ar gas mixture for oxidation measurements.

The chemical composition of the effluent gas after reaction was analyzed using a Balzers QMS200 quadrupol mass spectrometer. The analyzer was calibrated with gas mixtures of known composition so that a quantitative analysis of the reduction and oxidation was possible. The various reaction peaks in the concentration profiles were integrated after baseline substraction. The absolute amount of reacted gases was then quantified from the total gas flow.

In order to remove carbonate and hydrate adsorbates from the surface, the samples were pretreated by heating in 8% O_2/Ar at $T = 623$ K. In addition, a preliminary TPR measurement and reoxidation was performed and the data discarded, because the TPR profiles were found to become reproducible only after a first such cycle. Isothermal and temperature-programmed oxidation measurements were performed following TPR after cooling the sample in pure Ar.

3. RESULTS AND DISCUSSION

3.1. Temperature-Programmed Reduction

Figure 1 shows a typical reduction profile of an undoped ceria sample. A reduction peak with a maximum at $T = 780$ K could be observed and was well separated from a second continuous increase in the rate of reduction at higher temperatures. The origin of this distinct reaction was investigated by measuring samples of different specific surface area. In principle, one may assume contributions from both the bulk and the surface of cerium oxide nanoparticles to the integrated peak of hydrogen consumption. The first contribution would be proportional to the mass whereas the second would be proportional to the absolute surface area of a sample.

$$N_{H_2}^{tot} = \alpha \cdot M_{sample} + \beta \cdot A_{sample}, \quad [1]$$

where α and β are constants. Dividing Eq. [1] by the sample mass one obtains the linear relationship

$$\frac{N_{H_2}^{tot}}{M_{sample}} = \alpha + \beta \cdot \frac{A_{sample}}{M_{sample}}. \quad [2]$$

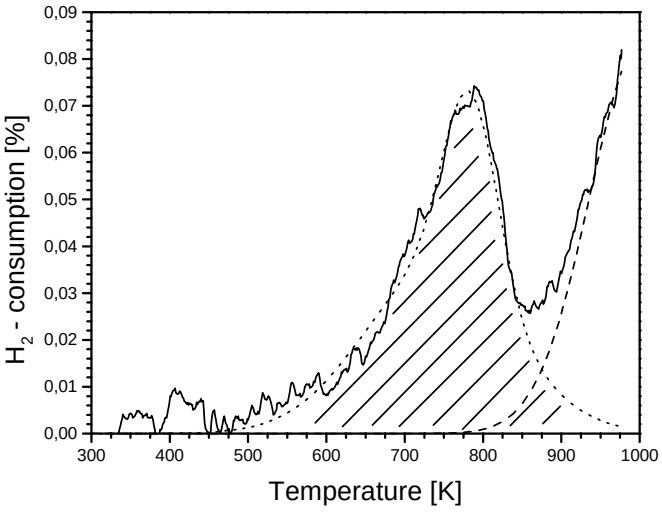

FIG. 1. Reduction profile of undoped ceria.

Ceria samples of different specific surface area were prepared by annealing nanocrystalline ceria at $T = 823$, 923, 973, 1023, and 1073 K. The results from the H_2 TPR measurements of these samples are plotted according to Eq. [2] in Fig. 2. Linear regression of the data yields an intercept $\alpha = 10.19 \pm 6.77$ μmol m^{-2} and a slope $\beta = 9.55 \pm 1.38$ μmol m^{-2}. This result indicates that the first reduction peak in Fig. 1 was dominated by the reduction of the ceria surface, in agreement with (19). The slope β of this analysis is a quantitative measure for the number of reactive sites per unit area of the surface of undoped ceria. By comparing the obtained value for β with the total concentration of formular units on a ceria surface, estimated by Bernal *et al.* (20) as 7.97 μmol m^{-2}, the degree of surface reduction can be roughly approximated by the following reaction:

$$CeO_2 + H_2 \rightarrow H_2O + CeO. \qquad [3]$$

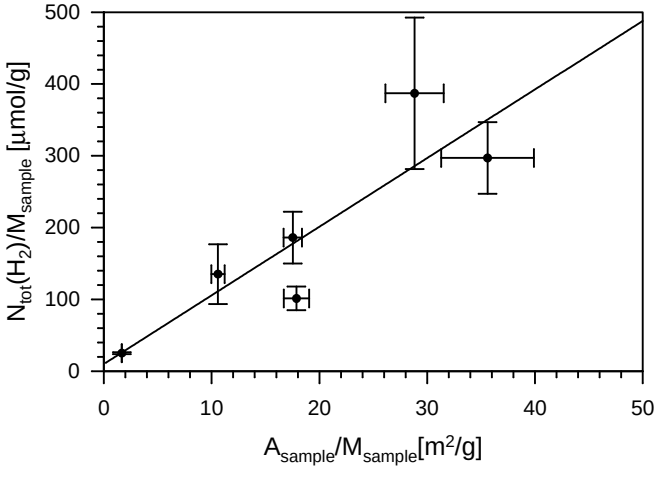

FIG. 2. H_2 consumption of the first reaction peak divided by the sample mass versus specific surface area of the ceria samples.

As mentioned in the experimental section, the TPR profiles of CuO/CeO_2 became reproducible only after a first preliminary measurement. The lack of reproducibility points to an irreversible change in the morphology of dispersed copper on the cerium oxide surface during the first reduction. A possible explanation for this effect could be redistribution of copper atoms if new sites of low energy become available during reduction. In order to obtain further information on the nature of this irreversible change, measurements of the local structure (e.g., using extended X-ray absorption fine structure (EXAFS)), will be necessary.

A typical TPR profile of a CuO/CeO_2 sample is shown in Fig. 3 together with the reduction profile of an undoped ceria sample for comparison. For CuO/CeO_2, the main reduction process was shifted to temperatures below 473 K. The profile shows a double peak structure with the first maximum at $T = 373$ K and the second at $T = 423$ K whereas the peak observed at 780 K in the TPR profile of pure ceria did not appear. A preliminary quantitative analysis revealed that the total hydrogen consumption was larger than the value expected for a complete reduction of the CuO component to Cu. The additional hydrogen consumption may be due to surface reduction at low temperature. In this case, the integrated double peak in the hydrogen consumption can be divided into one contribution proportional to the absolute amount of CuO in the sample and a second component proportional to the absolute surface area.

$$N_{H_2}^{tot} = \beta' \cdot A_{sample} + \gamma' \cdot N_{CuO}, \qquad [4]$$

with β' and γ' constants. Dividing Eq. [4] by the sample surface area yields a linear relationship:

$$\frac{N_{H_2}^{tot}}{A_{sample}} = \beta' + \gamma' \cdot \frac{N_{CuO}}{A_{sample}}. \qquad [5]$$

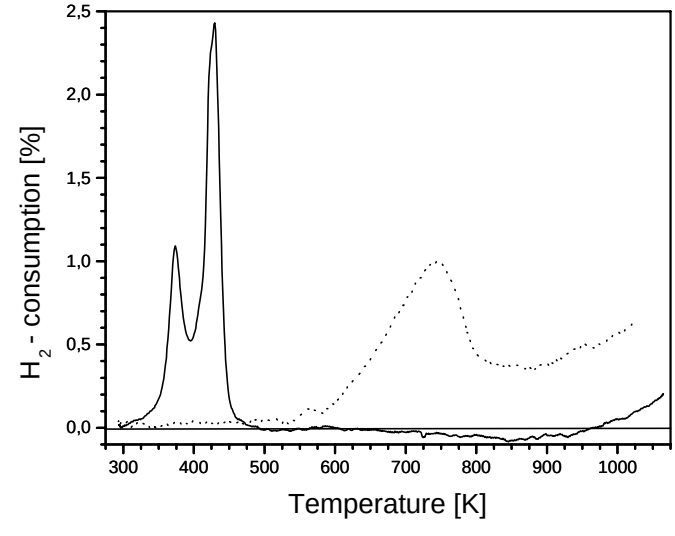

FIG. 3. H_2 TPR profiles of a 11.6% CuO/CeO_2 sample (solid line) and undoped ceria (dotted line).

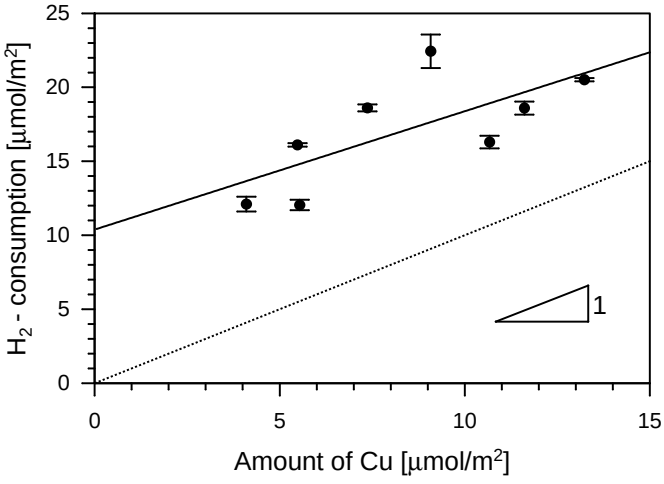

FIG. 4. H_2 consumption of the CuO reduction peak divided by the surface area as a function of the CuO amount in the samples per unit area. The solid line shows a linear fit of the data points; the dotted line represents the values expected for complete reduction of the CuO component.

As shown in Fig. 4, a linear regression analysis of the measured data yields an intercept $\beta' = 10.38 \pm 0.42$ μmol and a slope $\gamma' = 0.80$. The latter value indicates the degree of CuO reduction. Possible interpretations would be a complete reduction of 80% of the CuO to Cu or, alternatively, a complete reduction of 60% of the copper component and a partial reduction of the remaining 40% to Cu_2O. Both the intercept β' in this measurement and the slope β in Eq. [2] characterize the number of active sites per unit area of the cerium oxide surface and the two values were very close. Obviously, the surface reduction peak of undoped ceria at 780 K was not observed with CuO/CeO_2 because the reaction of hydrogen with the free surface was part of the low-temperature reaction. As only the consumption of hydrogen has been analyzed so far, it is not possible to distinguish surface reduction with a release of water from hydrogen adsorption on the cerium oxide surface. To clarify the nature of the low-temperature interaction between hydrogen and the cerium oxide surface, a TPR measurement was performed and also the water concentration in the effluent gas was analyzed (Fig. 5). There was no increase in the water signal ($m/e = 18$) corresponding to the H_2 consumption in the first peak at $T = 373$ K whereas the main peak of the H_2 consumption had an equivalent peak in the H_2O formation. The main reaction exhibited two peaks, at $T = 420$ and 420 K, which had been observed before (5). This was interpreted as a stepwise reduction in CuO: first the reduction from Cu^{2+} to Cu^{1+}, second from Cu^{1+} to Cu^0 (5, 6). Our result implies that the overall reaction of H_2 with CuO/CeO_2 involves the adsorption of hydrogen on all active sites of the cerium oxide surface and an almost complete reduction in the CuO component. The significant H_2 adsorption on CuO/CeO_2 was not observed with pure cerium oxide. In agreement with previous studies (5) our result indicates that the reduction properties of both constituent CuO and CeO_2 are strongly enhanced in the mixed catalyst compared to the pure materials.

As mentioned in the introduction, the oxidation of Cu on metal oxide supports by N_2O has been used to characterize the disperion of the copper component in prereduced supported CuO catalysts (13, 15). The method makes use of the different kinetics of surface and bulk oxidation of the copper clusters. When this method was applied to CuO/CeO_2 unphysical dispersions of more than 100% were obtained because the amount of N_2O consumed during oxidation was larger than the total copper component in the sample. The results of the previous section suggest that the excess is due to a reaction between N_2O and hydrogen which was adsorbed at the cerium oxide surface. Therefore, overall chemisorption of N_2O on prereduced CuO/CeO_2 is not selective. Nevertheless, it may still be possible to obtain information about the copper dispersion form N_2O oxidation if the contribution due to the reaction with adsorbed hydrogen could be separated. This was investigated by performing combined isothermal and temperature-programmed oxidation measurements.

3.2. Isothermal and Temperature-Programmed Oxidation

Isothermal oxidation of the sample, which is indicated by the formation of N_2, was observed at room temperature (Fig. 6). The reaction occurred in a sharp peak and the rate of reaction decayed to zero after about 500 s. Further oxidation was observed during the following TPO measurement. The TPO signal consisted of two overlapping but well-discernible peaks at 390 and 470 K. Quantitative analysis of the TPO profiles revealed a good agreement of the measured nitrogen formation and the amount of CuO in the various samples, as shown in Fig. 7. Therefore, the reaction occurring during TPO is associated with the oxidation of copper on cerium oxide. In contrast, the reaction of

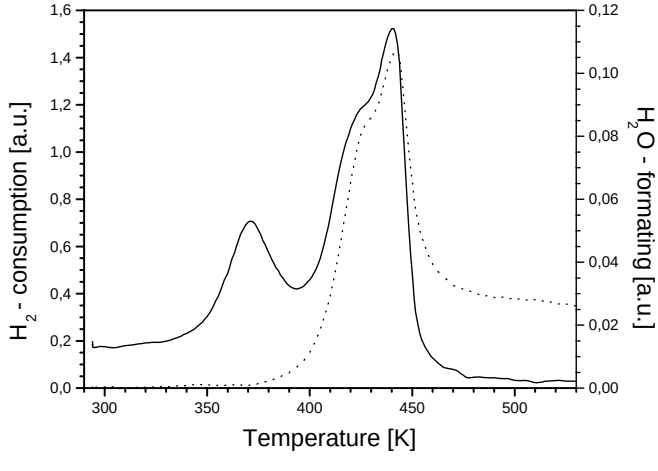

FIG. 5. Reduction profile of an 11.6% CuO/CeO_2 sample with an analysis of the H_2 signal (solid line) and water (dotted line).

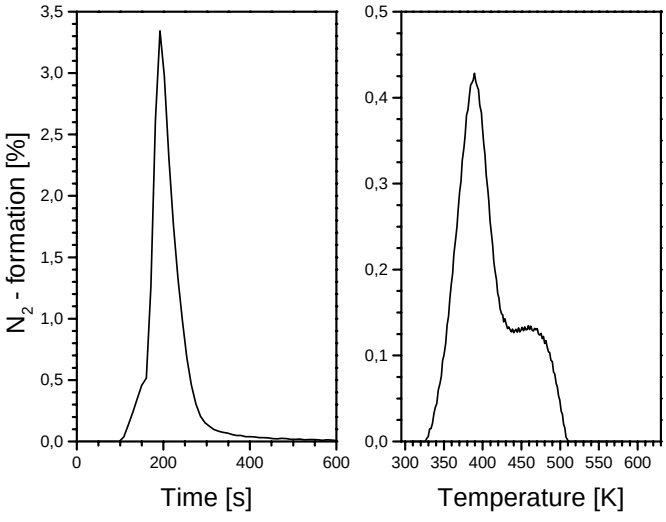

FIG. 6. N_2O oxidation of reduced 8.5% CuO/CeO_2. (Left) Isothermal oxidation; (right) TPO.

N_2O detected during the isothermal preoxidation at room temperature must be related to the oxidation of adsorbed hydrogen on the cerium oxide surface.

3.3. Morphology and Dispersion

As the reaction during N_2O TPO was identified as the oxidation of the reduced copper component on cerium oxide, we may now investigate the effect of the morphology of the copper particles on the TPO profile. The method of pulsed N_2O titration makes use of the much slower kinetics of bulk oxidation as compared to surface oxidation of copper clusters. If reduced copper clusters on an inert metal oxide support are exposed to N_2O under conditions at which the surface but not the bulk phase is oxidized, the dispersion of the copper clusters can be quantified by comparing the N_2O consumption with the total amount of copper in the sample. The TPO profile shown in Fig. 6 exhibits a double-peak structure which is associated with the oxidation of at least two different copper sites. In order to investigate whether the structure of the TPO profile was sensitive to the morphology and dispersion of copper on the cerium oxide substrate, a series of samples with identical composition of $Cu_{0.08}Ce_{0.92}O_{2-x}$ was prepared and changes in the structure and morphology were induced by heat treatment of the various specimens at high temperatures. The effect of the heat treatment is evident from a decrease in specific surface area from 90 $m^2\ g^{-1}$ after synthesis to 4 $m^2\ g^{-1}$ after annealing at $T = 1173$ K. Given the composition of $Cu_{0.08}Ce_{0.92}O_{2-x}$ we can estimate that the surface coverage with copper in the as-prepared sample was below one monolayer. With increasing annealing temperature, the surface area decreased considerably such that the copper component was forced to precipitate as a second phase. The formation of CuO- precipitates was observed in the XRD diagrams of samples which were annealed at temperatures above 1073 K (Fig. 8). It is important to notice that there was no indication of a second copper phase in the as-prepared sample. The only change observed in the diffraction pattern of samples annealed at temperatures below 1073 K was the narrowing of the cerium oxide diffraction peaks associated with a grain growth of the nanoparticles. Apparently, XRD was not sensitive to the dispersed copper component. However, the annealing treatment of the various samples even at low temperature did result in significant changes in the N_2O

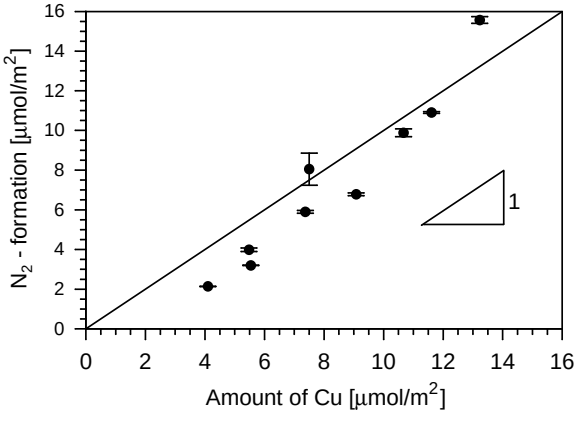

FIG. 7. Nitrogen formation per unit area of prereduced CuO/CeO_2 during N_2O TPO as a function of the CuO component per unit area (see Eq. [5]).

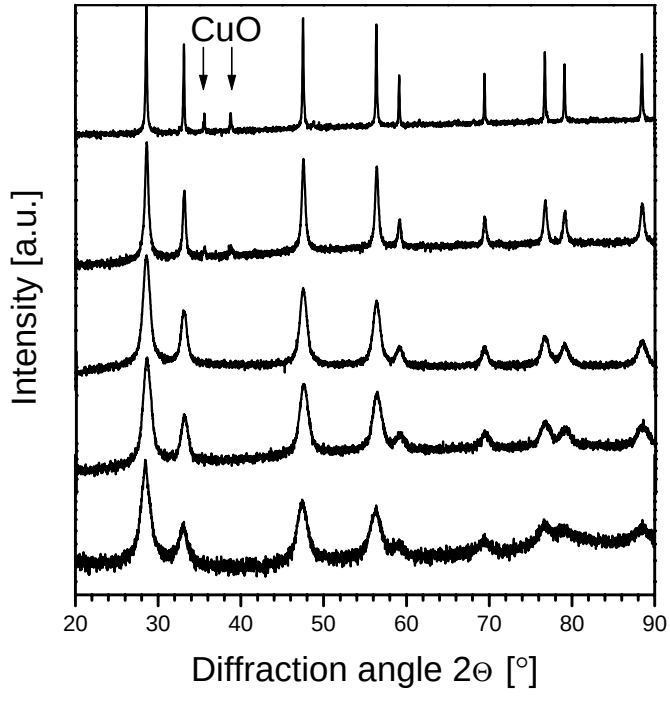

FIG. 8. X-ray diffraction pattern of the annealed $Cu_{0.08}Ce_{0.92}O_{2-x}$ samples. (Bottom to top) As prepared, annealed at 873, 973, 1073, and 1173 K. The peaks associated with the CuO phase are indicated.

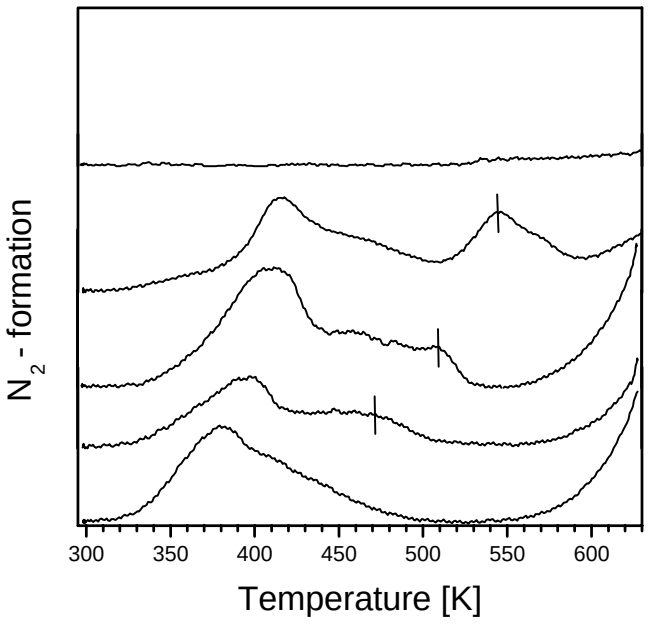

FIG. 9. TPO profiles of the annealed $Cu_{0.08}Ce_{0.92}O_{2-x}$ samples. (Bottom to top) As prepared, annealed at 873, 973, 1073, and 1173 K. The maxima of the increasing second peak are marked.

TPO profiles (Fig. 9). The TPO profile of the as-prepared sample exhibits a main oxidation reaction in the temperature range between 320 and 500 K, with a maximum at 380 K. A second increase in the N_2 concentration at $T = 553$ K indicated the beginning of a decomposition of N_2O, confirmed by a corresponding increase in the oxygen signal of the mass spectrometer. As a result of annealing at high temperatures, the TPO profiles of the $Cu_{0.08}Ce_{0.92}O_{2-x}$ samples evolved toward a double-peak structure with an additional shoulder at $T = 465$ K. The temperature of the second peak, marked in Fig. 9, shifted to higher temperature with increasing annealing temperature. These results suggest that considerable changes in the morphology of the dispersed copper component occurred in the sample, which were not resolved in the XRD measurements. It is suggested that the first peak, which did not shift in temperature, is associated with exposed copper ions whereas the second component may be related to copper ions, which are located below the surface. The fraction of this buried copper component increased with increasing annealing temperature, indicated by the enlarging intensity of the second peak. An alternative explanation for the double-peak structure of TPO profiles would be a stepwise oxidation from Cu^0 to Cu^{1+} and from Cu^{1+} to Cu^{2+}. However, if we assume complete reduction and oxidation in the initial and final state of the TPO, we would expect that both peaks exhibit the same integrated intensity, which was not observed. Therefore, we conclude that the TPO spectra in Fig. 9 point to a more complex morphology of dispersed Cu on the cerium oxide surface. Further details of the Cu sites may be explored by combined studies of TPO and EXAFS. It should be noticed that the temperature for bulk oxidation of larger Cu particles falls outside the range of TPO, as is evident from the sample annealed at 1173 K. The large particles of the precipitated copper phase could not be reoxidized at temperatures below 553 K (i.e., below the temperature at which decomposition of N_2O started). As a result, the temperature-programmed oxidation of prereduced copper in CuO/CeO_2 catalysts by N_2O is highly sensitive to the morphology of the copper component. Further studies, in particular using complementary techniques such as EXAFS, should help to obtain correlations between the TPO signals and structural units at the surface.

4. CONCLUSION

The reduction and oxidation properties of CeO_2 and mixed CuO/CeO_2 were studied by quantitative H_2 TPR and N_2O isothermal oxidation/TPO. The overall reaction of H_2 with CuO/CeO_2 involved the adsorption of hydrogen on all active sites of the surface and an almost complete reduction of the CuO component. The oxidation of the prereduced CuO/CeO_2 with N_2O could also be separated in partial reactions. At room temperature, the reaction of N_2O with the adsorbed hydrogen was observed, while the reaction during TPO was associated with the oxidation of copper on cerium oxide. Changes in the morphology and dispersion of CuO/CeO_2 induced by annealing treatment at high temperatures were found to have a strong effect on the N_2O TPO profile.

ACKNOWLEDGMENTS

The authors acknowledge financial support by the Fond der Chemischen Industrie and the Deutsche Forschungsgemeinschaft (SFB 277, "Grenzflächenbestimmte Materialien").

REFERENCES

1. Liu, W., and Flytzani-Stephanopoulos, M., *J. Catal.* **153**, 317 (1995).
2. Tschöpe, A., Liu, W., Flytzani-Stephanopoulos, M., and Ying, J. Y., *J. Catal.* **157**, 42 (1995).
3. Liu, W., and Flytzani-Stephanopoulos, M., *J. Catal.* **153**, 304 (1995).
4. Tschöpe, A., Schaadt, D., Birringer, R., and Ying, J. Y., *Nanostruct. Mater.* **9**, 423 (1997).
5. Hu, Y., Dong, L., Wang, J., Ding, W., and Chen, Y., *J. Mol. Catal. A* **162**, 307 (2000).
6. Kundakovic, Lj., and Flytzani-Stephanopoulos, M., *J. Catal.* **179**, 203 (1998).
7. Park, S., Vohs, J. M., and Gorte, R. J., *Nature* **404**, 265 (2000).
8. Tschöpe, A., and Ying, J. Y., *Nanostruct. Mater.* **4**, 617 (1994).
9. Tschöpe, A., Ying, J. Y., and Chiang, Y. M., *Mater. Sci. Eng. A* **204**, 267 (1995).
10. Tschöpe, A., and Ying, J. Y., *in* "Nanophase Materials" (R. W. Siegel and G. C. Hadjipanayis, Ed.), p. 781. Kluwer Academic, Dordrecht, 1994.
11. Knauth, P., Schwitzgebel, G., Tschöpe, A., and Villain, S., *J. Solid State Chem.* **140**, 295 (1998).

12. Tschöpe, A., Trudeau, M. L., and Ying, J. Y., *J. Phys. Chem. B* **42**, 8858 (1999).
13. Evans, J. W., Wainwright, M. S., Bridgewater, A. J., and Young, D. J., *Appl. Catal.* **7**, 75 (1983).
14. Scholten, J. J. F., *in* "Metal Surface Area and Metal Dispersion In Catalysts."
15. Scholten, J. J. F., and Konvalinka, J. A., *Trans. Faraday Soc.* **65**, 2456 (1969).
16. Chen, P.-L., and Chen, I.-W., *J. Am. Ceram. Soc.* **76** (6), 1577 (1993).
17. Olivier, J. P., and Conklin, W. B., *in* "International Symposium on the Effects of Surface Heterogenity in Adsorption and Catalysis on Solids." Kazimier Dolny, Poland, July 1992.
18. Olivier, J. P., *J. Porous Mater.* **2**, (1995).
19. Perrichon, V., Laachir, A., Bergeret, G., Frety, R., Tournayan, L., and Touret, O., *J. Chem. Soc. Faraday Trans.* **90** (5), 773 (1994).
20. Bernal, S., Calvino, J. J., Cifredo, G. A., Gatica, J. M., Perez Omil, J. A., and Pintado, J. M., *J. Chem. Soc. Faraday Trans.* **89** (18), 3499 (1993).